

The Pulsar Wind Nebula of G11.2–0.3

M. S. E. Roberts¹, C. Tam, V. M. Kaspi¹, M. Lyutikov¹

*McGill University, 3600 University St., Montreal, QC H3A 2T8,
Canada*

E. V. Gotthelf

Columbia University, 550 West 120th St., New York, NY 10027, USA

G. Vasisht

*Jet Propulsion Laboratory, Caltech, 4800 Oak Grove Dr., Pasadena, CA
91109, USA*

N. Kawai

RIKEN, 2-1 Hirosawa, Wako, 351-0198 Saitama, Japan

Abstract. We present high-resolution radio and X-ray studies of the composite supernova remnant G11.2–0.3. Using archival VLA data, we perform radio spectral tomography to measure for the first time the spectrum of the shell and plerion separately. We compare the radio morphology of each component to that observed in the hard and soft Chandra X-ray images. We measure the X-ray spectra of the shell and the emission in the interior and discuss the hypothesis that soft X-ray emission interior to the shell is the result of the expanding pulsar wind shocking with the supernova ejecta. We also see evidence for spatial variability in the hard X-ray emission near the pulsar, which we discuss in terms of ion mediated relativistic shocks.

1. Introduction

The supernova remnant G11.2–0.3 is a bright, circular X-ray and radio shell. At its center is the X-ray pulsar PSR J1811–1925 ($P = 65$ ms, spin-down energy $\dot{E} = 6.4 \times 10^{36}$ erg/s, characteristic age $\tau = 24,000$ yrs, Torii et al. 1999) and its associated hard X-ray wind nebula (Vasisht et al. 1996). The characteristic age is much greater than the apparent age of the SNR (~ 2000 yrs), the age implied by its highly centralized position within the remnant, and its likely association with the historical event of 386 A.D. (Kaspi et al. 2001). This discrepancy suggests the pulsar’s current spin period is very near its initial value, and that \dot{E} has remained nearly constant since the supernova explosion.

¹Department of Physics and Center for Space Research, MIT, Cambridge, MA 02139, USA

2. Radio and X-ray Analysis

Radio observations of G11.2–0.3 were made with the Very Large Array (VLA) at 20 and 6 cm between April 1984 and May 1985. To measure the spectral index α , where $S_\nu \propto \nu^{-\alpha}$, we spacially filtered the $u-v$ coverages to match spatial scales (Gaensler et al. 1999) by creating a model visibility data set from the 20 cm image with the $u-v$ sky distribution of the 6 cm data. A 20 cm image was then created from this model with identical parameters as the 6 cm image, and both were convolved with a $10''$ Gaussian. To determine spectral indices,

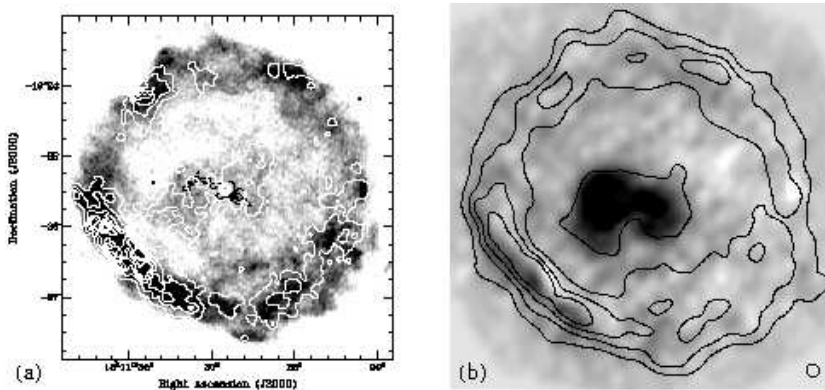


Figure 1. (a) High resolution image of G11.2–0.3 at 20 cm, with hard (black) and soft (white) X-ray contour overlays. (b) Tomographic difference image for $\alpha_t = 0.56$ at $10''$ resolution with 6 cm contours.

we used “spectral tomography” (Katz-Stone & Rudnick 1997). A difference image I_{α_t} was calculated by scaling the 6 cm image by a trial spectral index α_t , and subtracting it from the 20 cm image: $I_{\alpha_t} = I_{20} - (\nu_{20}/\nu_6)^{\alpha_t} I_6$, where I_{20} and I_6 were the images being compared, and ν_{20} and ν_6 were the average frequencies of the images. When the trial spectral index reached the actual spectral index of a particular feature, ie. $\alpha_t = \alpha$, that region appeared to vanish into the local background of the difference image (Figure 1). By examining the resulting series of difference images, we estimate $\alpha_P = 0.25 \pm 0.05$ for the PWN region in the center, while for the majority of the SNR shell we estimate a value of $\alpha_S = 0.56 \pm 0.02$, which is in agreement with single-dish radio results as published by Kothes & Reich (2001). However, the SNR shell appears to have a non-uniform spectral index, most noticeable in the south-eastern region. Negative residuals can be seen at $\alpha_t = 0.52$ in the outer component of the SNR shell, and lingering positive residuals appear at $\alpha_t = 0.58$ in the inner shell, indicating that the spectrum of the outer shell is slightly flatter, and the inner shell slightly steeper, than the bulk of the remnant.

Chandra observed G11.2–0.3 with the ACIS-S3 CCD on 2000 August 6 (obs 1) for 20 ks and 2000 October 15 (obs 2) for 15 ks. The analysis reported here was performed without the improved S3 FEF files, and we are currently re-analysing the data using the newer calibration. We created exposure corrected

“soft” band (0.6–1.65 keV) and “hard” band (4–9 keV) images to show regions of thermal and non-thermal emission, respectively. We extracted spectra from the regions indicated in Figure 2b. The interior background region was used when fitting features inside the shell and an exterior region as background for the shell (not shown).

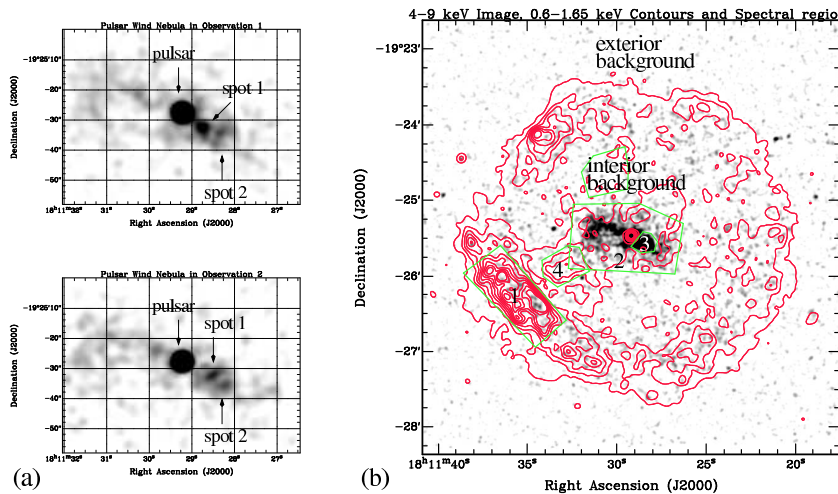


Figure 2. (a) Hard X-ray emission of PWN at epoch 1 (top) and epoch 2 (bottom). (b) Hard X-ray image with soft X-ray contours and spectral region designations.

We fit the shell region (1) and the soft “PWN” region (4) spectra to the VPSHock model plus absorption in XSPEC using spatially weighted response files, fitting for elemental abundances that could be constrained by the data. We added a power-law model when fitting region (1) due to an excess of hard photons in that region. The results suggest the region (4) spectrum is slightly cooler than region (1) ($kT \sim 0.42$ keV vs. $kT \sim 0.55$ keV) and has higher abundances of O, Ne, Mg, and S. For the hard PWN (regions 2 and 3), we fixed the VPSHock values from the region (4) fit, allowing only the normalization to vary and adding a power-law. The resulting photon spectral index was $\sim 1.5 \pm 0.2$ and the unabsorbed power-law flux of regions (2) (the entire PWN minus the pulsar) and (3) (the bright portion of the PWN) were $\sim 4.1 \times 10^{-12}$ erg cm $^{-2}$ s $^{-1}$ and 7.3×10^{-13} erg cm $^{-2}$ s $^{-1}$ respectively.

The hard band images from the two observation epochs show two bright “spots” in region (3) near the pulsar (Figure 2a). Assuming a distance of 5 kpc to the remnant, spot 1 is ~ 0.20 pc and spot 2 is ~ 0.34 pc from the pulsar. Between epochs, the centroided positions of the spots moved significantly away from the pulsar, implying space velocities of $\sim c$, with the relative velocity of spot 2 $\sim 2/3$ that of spot 1.

3. Discussion

The separation between the PWN and the inner edge of the shell in both radio and X-rays suggests that the remnant may not have reached the Sedov phase. This would imply the supernova ejecta within the shell, which interacts with the PWN, is still in the free expansion phase. The shell itself, however, has probably swept up enough mass to be between the free expansion and Sedov solutions. The expansion of the PWN into the ejecta is supersonic, and should set up a forward shock. This heats the ejecta, possibly resulting in the regions of thermal emission seen interior to the shell. The apparent symmetry around the pulsar of this soft “PWN” emission (region 4), along with the relatively greater abundances of heavy elements compared with the bright shell, support this picture. The radio PWN on the one side is sandwiched between the bright, narrow, jet-like hard X-ray feature and the soft “PWN” region, which also suggests a connection. Simple spherical models of PWN expansion (eg. Reynolds & Chevalier 1984) into the freely expanding interior of an SNR suggest that the ratio of the PWN radius to the SNR radius should be ~ 0.2 , assuming that the shell is also freely expanding into the ISM. The larger observed ratio of ~ 0.3 is expected if the shell has slowed due to accumulated ISM mass but the reverse shock has not yet encountered the PWN and compressed it.

The bright spots in the hard X-ray nebula may be the equivalent of the Crab’s “wisps”. The motion of wisps may be interpreted in the framework of ion mediated relativistic shocks (Gallant & Arons 1994). We can estimate σ (Kennel & Coroniti 1984), the ratio of Poynting to particle momentum flux in the wind from the expansion velocity of the PWN (assuming $d \sim 5$ kpc and an age of 1600 yrs) as $\sigma \sim V/c \sim 0.002$. We estimate the magnetic field in the shocked flow $B \simeq 3(\sigma \dot{E}/(4\pi r_s^2 c))^{1/2} = 3\mu G$ if we assume the position of the wind termination shock r_s is approximately that of spot 1. If we identify the distance between the two bright spots, with the ion gyration radius $r_{L,i}$, we find the ions have passed through $\sim 3\sigma^{1/2}r_{L,i}/r_s \sim 0.1$ of the total potential drop through the open magnetosphere, similar to the Crab’s value of 0.3. We conclude that both the geometry and dynamics (nearly relativistic motion) of the bright spots observed near PSR J1811–1925 are consistent with the ion mediated relativistic shock model of Gallant and Arons.

References

- Gaensler, B. M. et al. 1999, MNRAS, 305, 724
 Gallant, Y. A. & Arons, J. 1994, ApJ, 435, 230
 Kaspi, V. M. et al. 2001, ApJ, 560, 371
 Katz-Stone, D. M. & Rudnick, L. 1997, ApJ, 488, 146
 Kennel, C. F. & Coroniti, F. V. 1984, ApJ, 283, 694
 Kothes, R. & Reich, W. 2001, A&A, 372, 627
 Reynolds, S. P. & Chevalier, R. A. 1984, ApJ, 278, 630
 Torii, K. et al. 1999, ApJ, 523, L69
 Vasisht, G. et al. 1996, ApJ, 456, 59